Rare Metal Materials and Engineering
Volume 47, Issue 5, May 2018
Online English edition of the Chinese language journal

Available online at www.sciencedirect.com
ScienceDirect

Cite this article as: Rare Metal Materials and Engineering, 2018, 47(5): 1370-1376.

ARTICLE

Crack Propagation and Microstructural Evolution of Ni-based Single Crystal Alloy Under Shear Loads

Li Ben, Zhang Shiming, F. A. Essa, Dong Chao, Yu Jingui, Zhang Qiaoxin

Wuhan University of Technology, Wuhan 430070, China

Abstract: Crack propagation and microstructural evolution of Ni-based single crystal alloy were investigated under shear load by molecular dynamics simulations. Stress-strain, potential energy and crack growth rates were explored. Moreover, the influences of temperatures and strain rates on crack propagation were revealed. We find that the critical stress value increases with the decreasing temperature or increasing strain rate. As the temperature increases, the crack propagation is accelerated by severe thermal vibrations. Dislocations pile-up and twinning emerge at a higher strain rate, resulting in work hardening.

Key words: Ni-based single crystal alloy; crack propagation; microstructure evolution; shear loads; slip bands

Ni-based single crystal alloy, as increasingly important engineering materials, has been widely used in various industrial fields including aviation, spaceflight, navigation and other high technologies[1-4]. As an advanced aero engine alloy, it is finding a wide utilization in the development of casing and compressor blades due to its excellent high-temperature mechanical properties[5-9]. However, blades are susceptible to inside micro cracks in poor working conditions despite of their perfect external surfaces. These cracks will propagate and eventually lead to material failure under the coupling effects of thermal and mechanical loads. Moreover, the operational performances, life span and engineering applications of this superalloy are seriously affected. Generally, crack propagations are directly influenced by the dislocation slips and twinning modes[10-12]. Therefore, it is necessary to study the structural evolution regularity of nickel at atomic level to control and reduce the material fractures in subsequent processes.

Recent years have seen growing popularity of molecular dynamics (MD) simulations, which can model material evolution processes and provide detailed information about the deformation at microscopic scales [13-15]. For this reason, numerous studies have been conducted on crack propagations of nickel by MD simulations. Sung et al. [16] have investigated the effect of crystal orientations on crack propagations of nickel. It is found that the direction and path of crack propagation primarily depend on crystal orientation. Wu et al.[17] have explored the influence of temperatures on crack propagations in nickel-base alloys based on MD simulations. Results reveal that intense stress concentrations are of frequent occurrence at crack tips, which finally lead to the brittle fractures especially at low temperatures. Moreover, crack propagations take the initiative to display the brittle-to-ductile transition as the temperature increases. Potirniche et al.[18] have adopted MD simulations to perform a systematic study on nickel with different numbers of voids. It shows that material with a single void can possess much higher yield strength than the model of double voids, but the crack propagation rate with a single void is slower than that with double voids. Zhao et al. [19] have investigated the nickel plates containing both cracks and voids. It shows that the locations of voids have great effects on the crack initiation time. Karimi et al. [20] have also conducted a further study by MD simulations. It reveals that the vacancy near crack tip is able to enhance the stress field. As a result, the release rate of critical energy is decreased. Yu et al. [21] have analyzed the influences of crack locations on crack propagation

Received date: October 9, 2017
Foundation item: National Natural Science Foundation of China (51210008)
Corresponding author: Yu Jingui, Ph. D., School of Mechanical and Electronic Engineering, Wuhan University of Technology, Wuhan 430070, P. R. China, E-mail: yujingui@whut.edu.cn

behaviors in Ni/Ni_3Al interfacial materials. It is concluded that the yield stress of the intergranular crack model is greater than that of the transgranular crack model. Hocker et al.[22] have investigated the crack propagation behaviors at Ni/Ni_3Al interfaces by MD simulations. Results show that the interface termination plays an important role in crack morphology. It also suggests that the crack plane tends to be smooth in Ni terminated interfaces and the coarse surface appears in Al terminated interfaces. The above studies were carried out under tensile loads. However, few studies are implemented under the shear loads with different temperatures and strain rates, which is detrimental to reveal the crack propagation behaviors and microstructural evolution of Ni-based single crystal alloy.

In this research, we used MD simulations to study the fracture mechanisms and microstructural evolution of Ni-based single crystal alloy under shear loads. Meanwhile, influence of temperatures and strain rates on crack propagation behaviors were developed under shear loads. The microstructure evolutions, such as dislocation slip and twinning development, were also displayed in MD simulations. Finally, the variations of energy and crack length were used to describe the crack growth rates.

1 Computational Methods

MD simulations were implemented using the embedded-atom-method (EAM) potential developed by Yamakov[23]. Such potential can perfectly account for interatomic interactions. Thus it is widely adopted to explore the metals with face-centered cubic (fcc) structures. EAM potential (E) is composed of two parts and can be expressed as:

$$E=\sum_i G_i\left(\sum_{i\neq j}\rho_j^{\mathrm{a}}\left(r_{ij}\right)\right)+\frac{1}{2}\sum_{ij}U_{ij}\left(r_{ij}\right) \tag{1}$$

where G_i is the embedding energy of atom i, ρ_j^{a} is the averaged atomic electron density within a cutoff radius, r_i^j is the distance between atoms i and j, while U_{ij} is the potential between two atoms. Since the appropriate force fields are crucial to obtain accurate results in MD simulations, the atomic stress can be described using Virial theorem and von Mises theory. The Virial stress is given as:

$$\sigma_{\alpha\beta}(i)=-\frac{1}{2\Omega}\left[\sum_j F_{ij}^{\alpha}r_{ij}^{\beta}+2m_i v_i^{\alpha}v_i^{\beta}\right] \tag{2}$$

where Ω represents the original atomic volume, m_i and v_i refer to the mass and speed of atom i, respectively, F_{ij} and r_{ij} mean the force and displacement vectors between atoms i and j, respectively, the superscripts of α and β are coordinate components. Besides, von Mises stress is given by the following equation:

$$\sigma_e=\frac{1}{\sqrt{2}}\left[\begin{array}{l}\left(\sigma_x-\sigma_y\right)^2+\left(\sigma_y-\sigma_z\right)^2+\left(\sigma_z-\sigma_x\right)^2+\\ 6\left(\tau_{xy}^2+\tau_{xz}^2+\tau_{yz}^2\right)\end{array}\right]^{\frac{1}{2}} \tag{3}$$

where σ_x, σ_y and σ_z are the averaged stresses in x, y and z directions, respectively. in order to identify the microstructure evolution under shear loads, the center symmetry parameter (CSP) method was applied in MD simulations. CSP can be expressed as:

$$\mathrm{CSP}=\frac{1}{D_0^2}\sum_{j=1,6}\left|R_j+R_{j+6}\right|^2 \tag{4}$$

where R_j and R_{j+6} represent the lattice vectors of six nearest pair-bonds in system, and D_0 refers to the distance between two adjacent atoms. The value of CSP indicates the degree of lattice mismatch. The crystal structure is perfect when CSP is 0. But higher values of CSP mean more serious crystal damage.

The model was constructed with γ phase at upper layer and γ' phase at lower layer. x, y and z directions are the crystal orientations of [100], [010] and [001], respectively. As the lattice constants of γ and γ' phases are different, lattice mismatch certainly occurs at the grain boundary. In order to minimize the influence of mismatch on material, a reasonable lattice number was obtained by the method of coincidence site lattice (CSL). However, the original mismatch dislocations still existed at model interfaces. Herein, the system is modeled by two grains. One is the $134a_\gamma\times4a_\gamma\times33a_\gamma$ cubic box with Ni lattice constant a_γ and the other is the $132a_{\gamma'}\times4a_{\gamma'}\times33a_{\gamma'}$ cubic box with Ni_3Al lattice constant $a_{\gamma'}$ (Fig.1a). The initial crack is introduced by removing atoms from perfect crystal. The length of initial crack is $30\,a_\gamma$ and its width is $4\,a_\gamma$ (a_γ stands for the lattice constant of the corresponding phase, the initial crack lies in the middle of the model and the two phase interfaces). Atoms at four top and bottom layers of the model are fixed as loading planes, while the remaining atoms are performed as free parts and obeyed Newton's second law.

In order to alleviate the internal stress concentration and reduce energy, the model was equilibrated in a NVT ensemble (the number of particles N, volume V and temperature T of system are constant) with a constant time step of 1 fs. Four layers of atoms on the top and bottom of the model are fixed. The same strain rate with opposite direction is applied on the top and bottom four layers in Fig.1a. For the purpose of studying the influence of strain rates and temperatures on microstructure evolutions during crack propagations, different strain rates (0.01, 0.02 and 0.03 nm/ps) were set up. Moreover, simulations were carried out at 300, 600 and 900 K by a Nose-Hoover thermostat. The periodic boundary conditions were applied in y direction. And non-periodic boundary conditions were

assigned in x and z directions. The open source MD code LAMMPS[24], visualization tools Atomeye[25] and Ovito[26] were used in atomistic simulations.

2 Results and Discussion

2.1 Crack propagation and microstructural evolution under shear loads

Shear loads were applied with a constant strain rate of 0.01 nm/ps at 300 K to explore the crack propagation of pre-cracked Ni-based single crystal alloy. Fig.1 shows the atomic configurations with different strains. Dislocations firstly nucleate at crack tip where exists the stress concentration. As the strain increases, other stress concentration zones appear and lead to more dislocations. The initial crack starts to extend along dislocation slip plane, which greatly relaxes the stress concentration. A persistent slip band composed of dislocations occurs around the crack tip when the strain comes to 11.5% in Fig.1b. These dislocations are emitted from crack tips and eventually form slip bands under shear loads. The existence of slip bands in front of crack tips greatly relaxes stress concentrations and leads to further crack propagations. The dislocations ahead of crack tips gradually develop and become tight due to the increase of strains in Fig.1c. Meanwhile, persistent slip bands occur in the lower-left (Fig.1c) and upper-left (Fig.1d) corners of nickel-base single crystal in succession. Moreover, severe deformation is experienced by other persistent slip bands. Ultimately, crack significantly extends forward to each other until the material breaks. Besides, the magnified dislocations are also given in Fig.1b.

Fig.2 shows the stress-strain curve of Ni-based single crystal alloy with a strain rate of 0.01 nm/ps at 300 K. The mechanical response is linear elastic before 4.3%. Dislocations are emitted from crack tips when stress reaches the yield point of 5.08 GPa (Fig.2a). With more dislocations nucleating and moving in different planes, the systemic stress significantly decreases to about 2.76 GPa. Crack propagations are prevented due to lots of slip bands forming ahead of crack tips and the existence of dislocation pile-up, which can further contribute to the increase of stress (Fig.2b). The stress decreases again when a new crack surface emerges in lower-left corner (Fig.2c). Cracks extend forward (Fig.2d) until the fracture happens (Fig.2e).

The kinetic energy of the system keeps unchanged because temperature remains constant. It means that changes of total energy are simply determined by the potential energy. Due to the disorder atoms appearing at crack tips, emission of dislocations results in a slight energy reduction. However, the potential energy at this moment is lower than the critical value of the formation of new crack surfaces. In consequence, the system energy increases again, but its growth rate is lower than that in elastic stage. Once the system energy is able to overcome the fracture activation energy, vast potential energy is released. At the end of crack propagations, the potential energy slightly fluctuates around a certain value but is still greater than the initial energy. The reason is that the potential energy absorbed from shear loads is stored as surface energy due to the formation of new surface.

2.2 Effect of temperature on crack propagation and microstructural evolution

To fully understand the influence of temperature on crack propagation and microstructural evolutions under shear loads, the constant strain rate of 0.01 nm/ps at various temperatures was adopted to perform MD simulations. Snapshots of CSP at 300 K are shown in Fig.1, 600 K and 900 K are shown in Fig.3. At 300 K, slip bands near crack tips release lots of stresses. As the applied strain increases, slip bands successively emerge in lower-left corner, and finally evolve into crack propagation, resulting in material fractures.

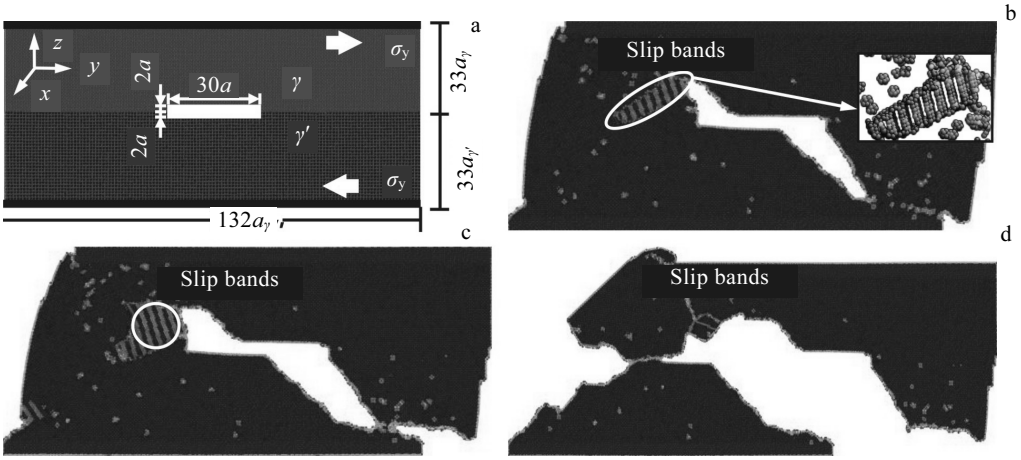

Fig.1 Crack propagation processes and distributions of CSP at 300 K with a strain rate of 0.01 nm/ps under various strains: (a) MD model, (b) 11.5%, (c) 16.5%, (d) 26.1%

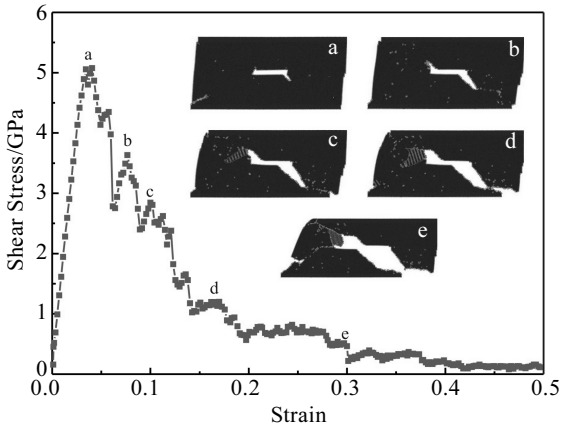

Fig.2 Stress-strain curve of nickel-base single crystal under shear loads

At 600 K, twinning nucleates at the upper-right corner of system in Fig.3b. Twinning gradually develops and finally encounters dislocations (Fig.3c) emitted from crack tips. As a consequence, movement of dislocations are obstructed and the material is strengthened. When the temperature is increased to 900 K (Fig.3d~3f), the critical shear stress of dislocation slip is small due to its higher mobility of atoms than that at 300 K. As dislocation network annihilates at the crack surface, the fracture surface at 900 K is rougher than that of 300 and 600 K. The above microstructural evolutions have proved that the temperature has a significant influence on crack propagations under shear loads.

The shear stress-strain curves are plotted for Ni-based single crystal alloy at three kinds of temperatures in Fig.4a. We find that the stress almost increases linearly at the elastic stage, and the initial slopes are independent of temperatures. But the yield strength decreases from 5.076 GPa to 3.939 GPa with the increasing temperatures from 300 K to 900 K. Dislocations are more likely to slip at higher temperatures. At 300 K, crack propagation is not blocked by slip bands ahead of crack tips. New crack surface is formed easily and quickly. At 600 K, the initial crack propagation is retarded by twinning and dislocation pile-ups. Therefore, the stress concentration is relaxed in a slow manner. At 900 K, the stress remains relatively stable for a long time until new dislocations are emitted from interfaces. The potential energy of the system as a function of strains is exhibited in Fig.4b. Fig.4b shows the potential energy with respect to strains at different temperatures. The trends of potential energy are roughly same, which also exist as fluctuant increasing processes until the fracture. Crack length is an important aspect to characterize crack growth and fracture behaviors, which is calculated by the crack length in *Y* direction. However, the real crack length is the path of crack propagation. The crack length as a function of strains at various temperatures is exhibited in Fig.4c. At 300 K, the initial crack extends rapidly. When the strain is between 9.2% and 29.8%, the crack grows slower because of the formed slip bands near crack tips. The crack length increases quickly again. When the strain exceeds 32.6%, the crack growth rate gradually decreases. At 600 K, the initial crack propagates slowly due to the hindrance of twinning. The crack propagation rate increases rapidly when the strain is greater than 37.9%. But such rate is still much lower than that of 300 K. At 900 K, owing to the high mobility of atoms, the stress of the driving crack tip declines sharply.

The crack growth accelerates until the strain reaches 32.6%, and it is still the slowest. It can also be clearly seen that the crack length is the shortest at 900 K.

2.3 Effect of strain rate on crack propagation and microstructural evolution

In order to clearly investigate the influence of shear strain rates on crack propagations, MD simulations were performed at 300 K with strain rates of 0.01, 0.02 and 0.03 nm/ps under shear loads. For the strain rate of 0.01 nm/ps in Fig.1, ladder-like dislocation slip bands emerge in

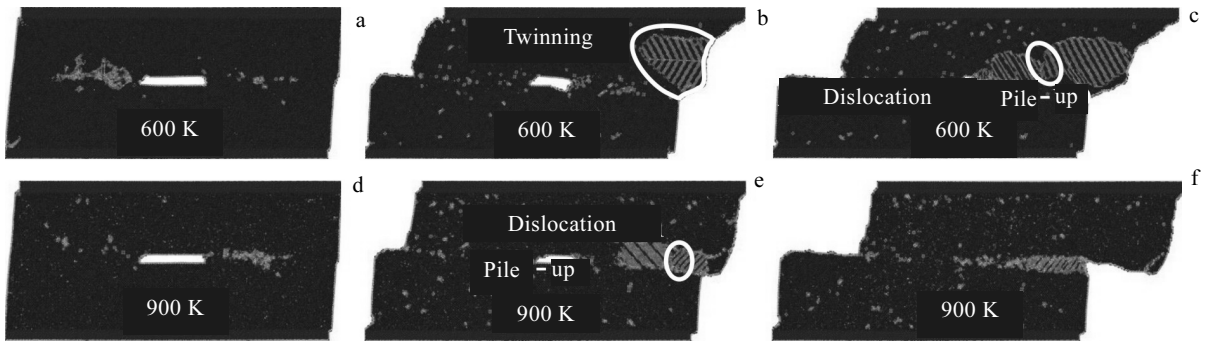

Fig.3 Crack propagation processes and distributions of CSP at 600 K and 900 K with a strain rate of 0.01 nm/ps under various strains: (a) 3.9%, (b) 25.3%, (c) 33.3%, (d) 3.2%, (e) 16.1%, and (f) 42.7%

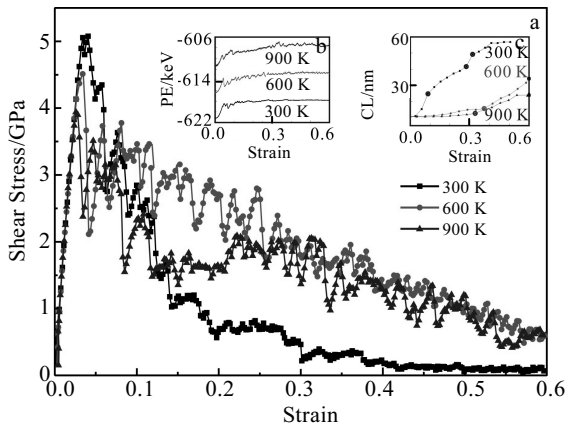

Fig.4 Relationship of strain with shear stress (a), potential energy (PE) (b), crack length (CL) (c) at different temperatures

front of crack tips. And then, similar slip bands successively appear in other stress concentration areas. With the increasing of strain, a new crack surface is formed in the lower-left corner of Ni-based single crystal alloy and then propagates forward.

Fig.5a~5d depicts the distribution of CSP at the strain rate of 0.02 nm/ps. We find dislocations are emitted from crack tips, and the density of dislocations is higher than the case of 0.01 nm/ps. The original crack propagates along the slip plane under shear loads. Lots of voids arise at stress concentration areas and gradually enlarge. Thereafter, voids connect with each other, which greatly promotes the crack propagations. Owing to few obstacles but multiple voids appearing in slip planes, the Ni-based single crystal alloy is completely broken under the smallest strain. Fig.5e~5h depicts the distributions of CSP at the strain rate of 0.03 nm/ps. Twinning emerges in stress concentration areas locating in the upper-right corner when strain increases to 9.28% in Fig.5f. Twinning gradually distorts and disappears under shear loads. As the strain continues to increase, dislocations emit from lower-left corner. Then, crack tips move and encounter with each other near the interfaces in Fig.5g. The initial crack propagation is hindered by the resultant dislocation pile-up in Fig.5h. Meanwhile, twinning appears again near the interfaces. The formation of twinning can strengthen the Ni-based single crystal alloy and retard the crack propagation. It can be found that the final crack path is more zigzag than the cases of 0.01 nm/ps and 0.02 nm/ps. Besides, the generation and development of the magnified twinning are also given in Fig.5f and Fig.5h.

Fig.6a shows the shear properties of nickel-base single crystal with various strain rates. We find the strain rate has a remarkable impact on shear properties. Young's modulus is insensitive to strain rates, but the yield strength increases with strain rates due to the strain hardening mechanism.

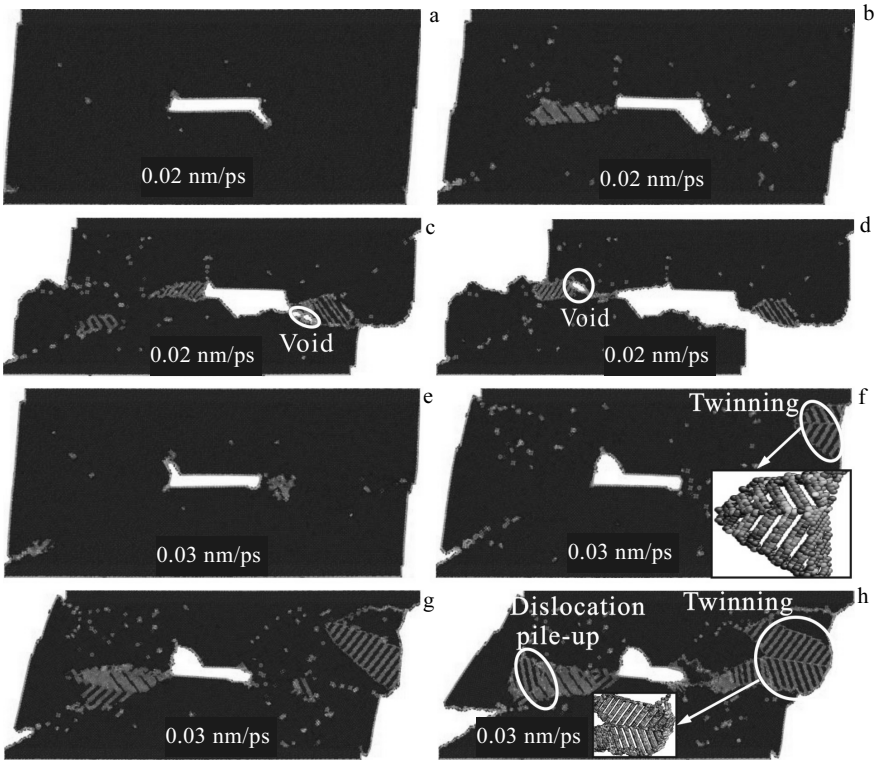

Fig.5 Crack propagation processes and distributions of CSP at 300 K with a strain rate of 0.02 nm/ps (a~d) and 0.03 nm/ps (e~h) under various strains: (a) 3.5%, (b) 6.8%, (c) 20.5%, (d) 36.6%, (e) 4.3%, (f) 9.3%, (g) 16.4%, and (h) 24.6%

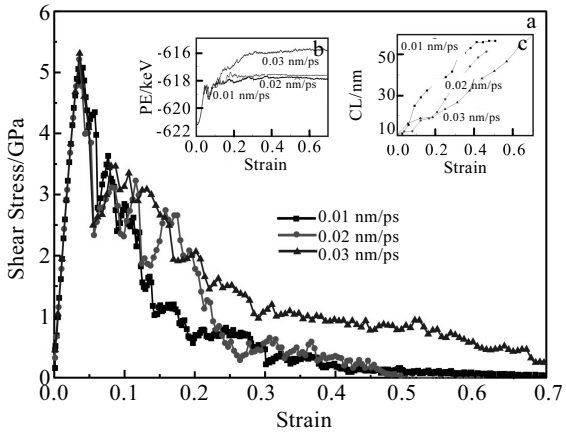

Fig.6 Relationship of strain with shear stress (a), potential energy (b), and crack length (c) under different strain rate conditions

After reaching the peak stress point, the stress resistance decreases abruptly due to the plastic deformation. Our simulation result is well in accordance with the result obtained by Sung et al [16].The persistent slip band ahead of crack tip hinders crack extension when the strain reaches 6.5% at the strain rate of 0.01 nm/ps. The stress-strain curve fluctuates when the strain increases from 6.8% to 20.5% at the strain rate of 0.02 nm/ps. It can be observed that the stress decreases because of the dislocation emission. When the strain exceeds 20.5%, stress drops dramatically due to the formation of dislocation slip planes. The dislocation and twinning successively emerge in stress concentration areas at the strain rate of 0.03 nm/ps. Dislocation slip tends to weaken the material strength while twinning strengthens the material. However, dislocation slip plays a dominant role at the strain rate of 0.03 nm/ps, which contributes to a fluctuant downward trend of stress. Compared with the strain rates of 0.01 nm/ps and 0.02 nm/ps, stress response exhibits the slowest declining tendency and fracture strain is the highest at the strain rate of 0.03 nm/ps. The potential energy as a function of strains at different strain rates are plotted in Fig.6b. There are a few differences between these energy-strain curves in the elastic region. The potential energy increases with the strain rate after reaching yielding points. Besides, the crack path at the strain rate of 0.03 nm/ps is the curviest in Fig.6b. Fig.6c depicts the crack length as a function of strain at different strain rates under shear loads. The crack length increases dramatically after yield at the strain rate of 0.01 nm/ps. Then, the crack propagations are hindered when the strain is between 9.3% and 29.8%. Crack propagates rapidly when initial crack overcomes obstacles and a new crack surface emerges in the lower-left corner. When it approaches to the breakage verge, the crack growth rate gradually decreases. Crack growth rate rises with fluctuations before the strain reaches 20.5% at the strain rate of 0.02 nm/ps. Then the formation of voids significantly promotes crack propagations until the material fractures. And the final crack length is the shortest one in the three cases. When the strain rate is 0.03 nm/ps, crack extension rate is greater than other cases in the early stage. However, the formation of dislocation pile-up and twinning restrains the crack to extend. Hence, the crack propagates forward at a low speed until the fracture.

3 Conclusions

1) MD simulations have been used to investigate the crack propagations and microstructural evolutions of Ni-based single crystal alloy under shear loads The initial slopes of stress-strain are insensitive to temperatures and strain rates under shear loads. With the increasing temperatures, the critical stress decreases due to the softening of Ni-based single crystal alloy at high temperatures. While the potential energy response increases and exhibits a severe fluctuation. As the strain rate increases, the yield strength increases due to the strain hardening mechanism.

2) Microstructural evolutions are quite different at various temperatures under the shear loads. At 300 K, there are few obstacles during crack propagations, and the crack length increases rapidly. At 600 K, the formation of twinning greatly strengthens the material resulting in a slow crack propagation. The crack propagation accelerates at 900 K due to the fast movement of dislocations. However it is still the slowest one among the three cases because the crack is passivated at high temperature.

3) The crack length growth rate is quite rapid at the strain rate 0.01 nm/ps. But a number of voids emerge inside material at the strain rate 0.02 nm/ps, which significantly promotes the crack extension at the late shearing stage. Twinning and dislocations emerge and compete between them at the strain rate of 0.03 nm/ps.

References

1 Marchetti L, Perrin S, Jambon F *et al*. *Corrosion Science*[J], 2016, 102: 24

2 Arias-González F, Val J D, Comesaña R *et al*. *Applied Surface Science*[J], 2016, 374: 197

3 Emmerich T, Schroer C. *Corrosion Science*[J], 2017, 120: 171

4 Semenov S G, Getsov L B, Tikhomirova E A *et al*. *Metal Science & Heat Treatment*[J], 2016, 57(11-12): 731

5 Graverend Jean-Briacle, Jacques Alain, Cormier Jonathan *et al*. *Acta Materialia*[J], 2015, 84: 65

6 Wu R, Sandfeld S. *Scripta Materialia*[J], 2016, 123: 42

7 Ning L, Zheng Z, Jin T *et al*. *Acta Metallurgica Sinica*[J], 2014, 50(8): 1011

8 Wen Z X, Zhang D X, Li S W *et al*. *Journal of Alloys and Compounds*[J], 2017, 692: 301

9 Wen Z X, Pei H Q, Wang B Z *et al*. *Materials at High Temperatures*[J], 2016, 33: 68
10 Qiao H, Agnew S R, Wu P D. *International Journal of Plasticity*[J], 2015, 65: 61
11 Fan H, Aubry S, Arsenlis A *et al*. *Scripta Materialia*[J], 2016, 112: 50
12 Min X, Emura S, Meng F *et al*. *Scripta Materialia*[J], 2015, 102: 79
13 Chen B, Diao Z J, Zhao Y L *et al*. *Fuel*[J], 2015, 154(5): 114
14 Yu F, Wang D, Xu X *et al*. *European Journal of Medicinal Chemistry*[J], 2017, 127: 493
15 He Y, And T R L, Ediger M D *et al*. *Macromolecules*[J], 2004, 37(13): 5032
16 Sung P H, Chen T C. *Computational Materials Science*[J], 2015, 102: 151
17 Wu W P, Yao Z Z. *Strength of Materials*[J], 2014, 46(2): 164
18 Potirniche G P, Horstemeyer M F, Wagner G J *et al*. *International Journal of Plasticity*[J], 2006, 22(2): 257
19 Zhao L G, O'Dowd N P, Busso E P. *Journal of the Mechanics & Physics of Solids*[J], 2006, 54(2): 288
20 Karimi M, Roarty T, Kaplan T. *Modelling & Simulation in Materials Science & Engineering*[J], 2006, 14(8): 1409
21 Yu J G, Zhang Q X, Liu R *et al*. *RSC Advances*[J], 2014, 4(62): 32 749
22 Hocker S, Schmauder S, Kumar P. *The European Physical Journal B*[J], 2011, 82(2): 133
23 Yamakov V I, Warner D H, Zamora R J *et al*. *Journal of the Mechanics & Physics of Solids*[J], 2014, 65(5): 35
24 Plimpton S, Crozier P, Thompson A. *Journal of Applied Physics*[J], 2015, 2(20): 4740
25 Li J. *Modelling and Simulation in Materials Science and Engineering*[J], 2003, 11: 173
26 Stukowski A. *Modelling and Simulation in Materials Science and Engineering*[J], 2010, 18: 015 012

剪切载荷条件下镍基单晶合金裂纹扩展与微观结构演化行为研究

李　本，张世明，F. A. Essa，董　超，余金桂，章桥新
（武汉理工大学，湖北 武汉 430070）

摘　要：利用分子动力学方法研究了镍基单晶合金在剪切载荷下的裂纹扩展和微观结构演化，分析了应力-应变、势能和裂纹生长速率的变化。同时，揭示了温度和剪切应变率对裂纹扩展和微观结构演化的影响。结果表明，临界分切应力随温度的降低和应变速率的增大而增大；随着温度的升高以及剪切载荷下发生剧烈的热运动，裂缝表现为加速扩展的趋势；而在较高的应变率影响下，会形成位错塞积和孪晶，出现加工硬化现象。

关键词：镍基单晶合金；裂纹扩展；微结构演化；剪切载荷；滑移带

作者简介：李　本，男，1986 年生，博士生，武汉理工大学机电工程学院，湖北 武汉 430070，E-mail：li_dd21@163.com